

Spherical Stellarator Configuration

Paul E. Moroz

*University of Wisconsin, Madison, Wisconsin 53706
and Lodestar Research Corporation, Boulder, Colorado 80301*

(Received 2 February 1996)

A novel ultralow aspect ratio stellarator system that can be called a spherical stellarator (SS), in analogy with the spherical tokamak concept, is considered. The coil configuration of a simplest SS differs from that of a spherical tokamak by inclination of the external parts of the toroidal field coils. This system possesses many attractive properties including compact design and coil simplicity, good access to the plasma, closed vacuum flux surfaces with large enclosed volume, significant external rotational transform, strong magnetic well, and simple divertor configuration. [S0031-9007(96)00759-4]

PACS numbers: 52.55.Hc, 52.55.Fa

Tokamaks and stellarators are two leading systems in the controlled fusion program via magnetic plasma confinement. The best plasma parameters have been obtained in the largest tokamaks: JET [1], TFTR [2], JT-60 [3], and some others. Tokamak operations with tritium plasmas carried out in TFTR [2] and JET [1] demonstrated significant fusion energy output. Stellarators are presently somewhat behind in their development. Nevertheless, the large stellarator devices are presently under construction in Japan [Large Helical Device (LHD) [4]] and in Germany [Wendelstein 7-X (W7-X) [5]].

Recently, strong interest has appeared in a compact tokamak design, where a single central post replaces the central parts of all toroidal field (TF) coils. This low aspect ratio (LAR) tokamaks with $A = 1.5-2.5$, (where A is the aspect ratio, i.e., the ratio of the average major radius to the average minor radius for the last closed flux surface), or ultralow aspect ratio (ULAR) tokamaks, with $A = 1.05-1.5$, are promising for obtaining plasmas with the high number density and high β (β is the ratio of thermal plasma energy to the magnetic field energy) in a device of moderate size and relatively low magnetic field. Good plasma access is another advantage of these configurations. The LAR or ULAR tokamaks are often called the spherical tokamaks (ST). The results reported from the spherical tokamaks START at Culham [6] and CDX-U [7] were very promising. In addition to the relatively high β obtained, low plasma disruptivity has been reported. Because of this initial success, the program on spherical tokamaks is quickly extending [8].

Some difficulties of the ST program are related to the fact that, because of tight space for the Ohmic current transformer, it cannot support the inductive current for a long time. Other, noninductive current drive (CD) methods [such as radio-frequency (RFCD) or neutral beam injection current drive (NBCD)] have to be used to maintain the plasma current beyond the initial Ohmic start-up. Another set of potential problems of the ST approach, as a next-step device or especially as a prototype for the fusion

reactor, are related to the fact that there is not enough space, between the central post (or the central transformer) and the plasma edge to protect it from the intense fluxes of heat, particles, and neutrons that can quickly damage the post.

Normally stellarators have large aspect ratios of $A \geq 10$. The lowest aspect ratio stellarators ever built are the Compact Helical System (CHS) [9] and the Compact Auburn Torsatron (CAT) [10] which have $A \approx 5$. Even the stellarators with $A \approx 7.5$, such as Advanced Toroidal Facility (ATF) or LHD, are called [11] low aspect ratio stellarators. Because the compact stellarator configuration is very attractive for a reactor design, there are a number of publications addressing compact stellarator issues [11-13], but again for the aspect ratios that cannot be called LAR or ULAR.

In this paper, we study the LAR or ULAR approach but, in contrast with the above mentioned tokamak systems, for a stellarator. We call such stellarators "spherical stellarators" (SS) in analogy with the spherical tokamaks. The coil configuration of SS has many common characteristics with that of ST. The simplest SS can be obtained by inclination of the external parts of all TF coils by the same angle. Similar to ST, it might have a central post combining the central parts of all TF coils. The main difference from ST is that the outboard parts of the TF coils in SS are nonplanar (like in a stellarator). We use the following definition of the aspect ratio in SS: $A = (R_{\max} + R_{\min})/2\langle r_p \rangle$. Here a symbol $\langle \rangle$ means averaging over the poloidal ϑ and toroidal φ angles. The value of $r_p(\vartheta, \varphi)$ is the minor radius on the last closed flux surface for given (ϑ, φ) , and R_{\max} , R_{\min} are the maximum and minimum major radii for the last closed flux surface. In some SS devices that we have considered, thus defined A was close to 1, although for more optimized cases (with the divertor coils, for example), A is usually about 1.5-2.

The following set of SS configurations is under discussion in this paper. The SS device is obtained from the corresponding ST configuration by rotation of the top parts of

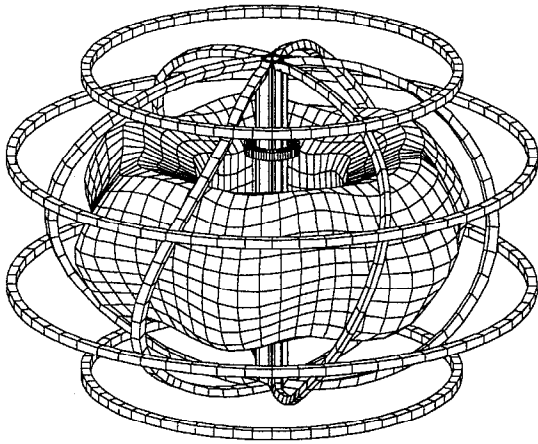


FIG. 1. Principle configuration of a spherical stellarator (SS). Shown are the coil system and the last closed flux surface.

the TF coils, relative to their bottom parts, at the toroidal angle $\Delta\varphi$. Thus the external parts of the modified TF coils are inclined (see Fig. 1). Good results were obtained for $\Delta\varphi = \pi/N$, where N is the number of TF coils in ST. In some sense, this type of SS configuration is similar to a device with inclined coils described in our recent publications [14–17], but corresponds to the ultralow aspect ratio. In this paper we are using D-shaped coils. Similar to a device with inclined coils, the SS of the type considered requires a set of poloidal field coils to compensate the vertical magnetic field produced by the inclined parts. The SS configuration with six TF coils (modified as described above) is shown in Fig. 1. The last closed flux surface can be seen as well. The poloidal cross section of the last closed flux surface is presented in Fig. 2, together with the

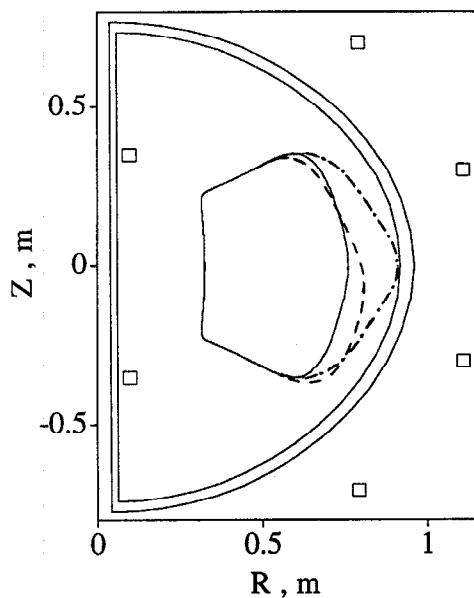


FIG. 2. Projection of the coil system of the SS device of Fig. 1 on the poloidal cross section. Shown also are the cross sections for the last closed flux surface at toroidal angles $\varphi = 0$ (solid curve), $\pi/2N$ (dashed), and π/N (dot-dashed).

coil projections, so the particular dimensions of the coils, chosen for this example, can be seen as well. Two poloidal field (PF) coils at small radii, whose projection is shown in Fig. 2 at the major radius $R = 0.1$ m, are introduced specially to demonstrate the simplicity of the divertor in this configuration. For the magnetic field $B \approx 0.7$ T at the middle of the last closed flux surface (at $R \approx 0.55$ m) the currents in the coils were as follows: $I_{TF} = 300$ kA (current in each TF coil), $I_{P1} = 60$ kA (current in each PF coil at $R = 1.12$ m), $I_{P2} = 35$ kA (current in each PF coil at $R = 0.8$ m), $I_{P3} = -40$ kA (current in each divertor coil at $R = 0.1$ m). Without these two divertor coils, the aspect ratio will be smaller: It will change from $A \approx 1.9$ to $A \approx 1.4$ for the configuration without the divertor coils (see Fig. 3). However, without the divertor, the significant particle and heat fluxes might be deposited on the central post (the similar problem as in ST devices). In SS, particle losses will occur mostly on the outboard parts of the flux surfaces, where the local magnetic field ripple is strongest. Details of the simple divertor configuration produced by the two mentioned PF coils are presented in Fig. 4. The field line traces show clearly that trajectories of the particles, leaving the last closed flux surface while being on its outboard part, will be directed by the divertor coils into the top and bottom areas where the divertor plates can be conveniently installed.

One can see that the divertor configuration in this kind of stellarators possesses toroidal symmetry (similar to that in a tokamak) and is significantly much simpler than the divertor configuration for any other stellarator (see, for example, [5] for a divertor in W7-X). Figure 4 shows also that the divertor region in SS is practically “ideal,” similar to that in a tokamak, without stochastic regions and magnetic islands which are so typical for stellarators.

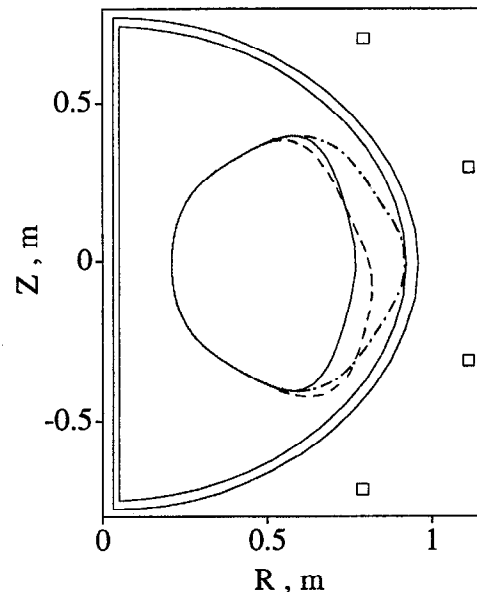


FIG. 3. Same as Fig. 2 but for the SS configuration without the divertor coils.

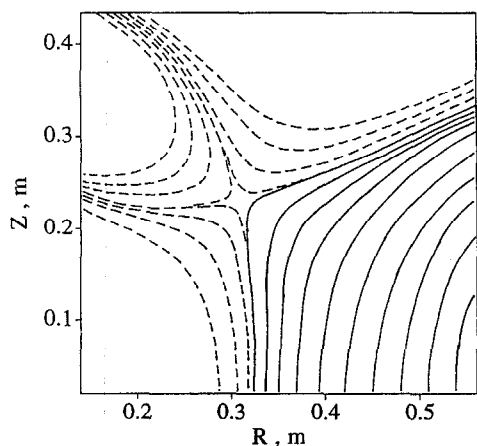


FIG. 4. Field line traces demonstrating the divertor configuration. Solid curves correspond to the closed flux surfaces, dashed curves show the opened field lines.

It is important to note, also, that the magnetic configuration obtained is favorable for magnetohydrodynamic (MHD) stability. It possesses a strong magnetic well, which can be defined through the integral $U = \int dl/B$ taken along field line and averaged over the flux surface. The average of the integral U can be expressed through the derivative of the enclosed volume V over the enclosed toroidal magnetic flux Φ [18]: $\langle U \rangle = dV/d\Phi$. The magnetic configuration is favorable to MHD stability if $\langle U \rangle$ decreases with the average minor radius ρ . The relative deepness of the magnetic well can be defined as $W(\rho) = 1 - \langle U(\rho) \rangle / \langle U(0) \rangle = 1 - V'(\Phi(\rho)) / V'(0)$, where $U(0)$ and $V'(0)$ correspond to the values at the magnetic axis, and $U(\rho)$ and $V'(\Phi(\rho))$ to the values at the given flux surface with the average minor radius ρ . Figure 5 shows (solid curve) the dependence of $W(\rho)$ for the SS configuration of Fig. 1 that corresponds to a total magnetic well of about $W_t = 67\%$. This is a very high number ensuring the good stability properties of the SS configuration.

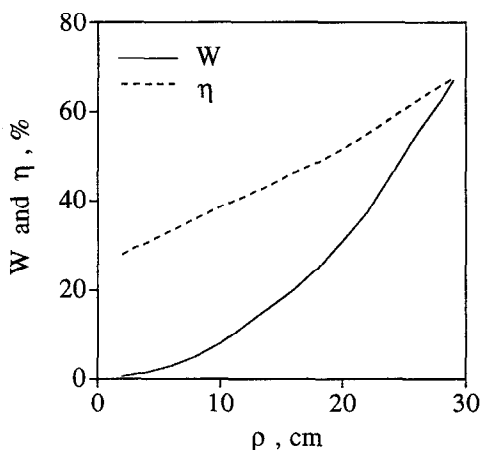


FIG. 5. Radial dependence of the magnetic well W and the magnetic field variation η .

The amount of trapped particles and particle transport in the device depend significantly on variation of $|B|$ along field lines. It can be characterized by the magnetic field modulation: $\eta(\rho) = (B_{\max} - B_{\min}) / (B_{\max} + B_{\min})$. The radial dependence of $\eta(\rho)$ for the device considered is presented in Fig. 5 (dashed curve). One can see that η is a growing function of ρ , and $\eta_{\max} \approx 67\%$ at the outermost flux surface with $\rho \approx 29$ cm. This value of the field modulation is less than in a typical ST device.

Rotational transform behavior in SS is very different from that in a typical stellarator. Figure 6 shows the radial dependence of the rotational transform $\iota = 1/q$, q being the safety factor, for the device of Fig. 1. As one can see, the total rotational transform ι (solid curve) is a decreasing function of ρ , which is typical for tokamaks and is very rare in stellarators. In SS, the local ι changes significantly in the poloidal direction: It is relatively large (dashed curve in Fig. 6, showing increasing ι_{ex} with ρ) on the external (outboard) halves of the flux surfaces, which are closer to the inclined parts on the coils, and small on the internal (inboard) halves of the flux surfaces (dotted curve, for ι_{in}). The relation between the total ι and its external ι_{ex} and internal ι_{in} components can be expressed as $2/\iota \approx 1/\iota_{\text{ex}} + 1/\iota_{\text{in}}$. The relatively large value of ι_{ex} , between 0.2 and 0.3, and the corresponding shear are of importance for good plasma equilibrium and stability properties in SS.

The SS configuration depends significantly on the number N of the TF coils. The change in the aspect ratio, A , and the central rotational transform $\iota(0)$ is given in Fig. 7 (for SS configurations without a divertor) for variation of N from 3 to 12. The case of $N = 6$ corresponds to Fig. 3 and represents probably a reasonable compromise. The SS configurations with a divertor, as mentioned above, have larger aspect ratios, but the general dependence on N is similar.

The SS configuration considered possesses wide flexibility and might feature many advantages. It can even

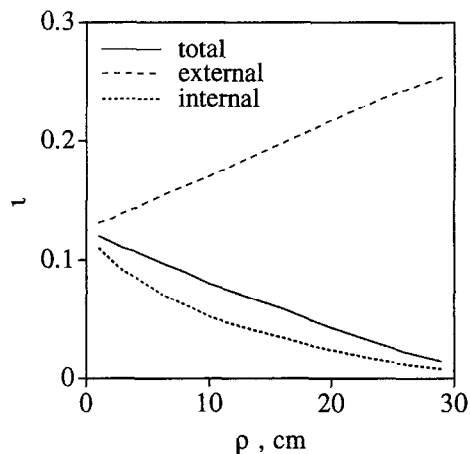


FIG. 6. Radial variation of the total rotational transform (solid curve) and its external (dashed) and internal (dotted) components.

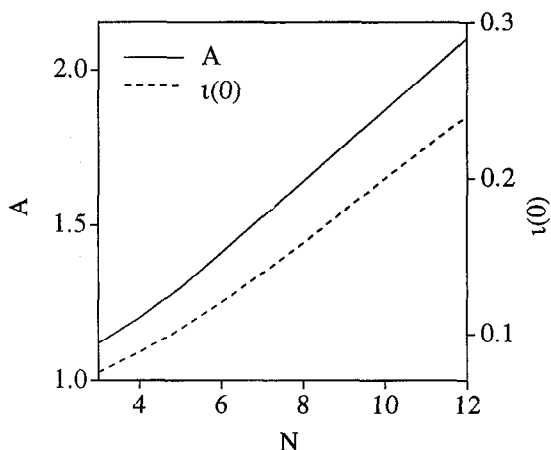


FIG. 7. Dependence of the plasma aspect ratio A and the central rotational transform $\iota(0)$ in SS on the number of TF coils N .

be converted into a novel stellarator-tokamak hybrid by adding (similar to that for ST) the standard ohmic current transformer. The aspect ratio A for SS is generally larger than that for ST. If one will try to increase A in ST, he will lose many benefits of ST. Contrary to that, the configuration of SS with a divertor, presented in Fig. 3, has $A = 1.9$ and there is enough space available near the central post not only for the transformer but also for installation of the protection and the blanket (for a reactor).

A few potential advantages of the SS configuration considered, over other approaches in controlled fusion via magnetic confinement, can be summarized as follows: (a) very compact design offering the low cost approach; (b) as a stellarator, it has closed vacuum flux surfaces ensuring efficient noninductive startup, and it does not need, in principle, the ohmic current transformer; (c) simple modular coil system; (d) easy access to the plasma; (e) more area for heat removal and the tritium breeding blanket in a reactor; (f) simple toroidally symmetric divertor configuration; and (g) enough space between the central post and the plasma surface to put the blanket and protect the post from the intense fluxes of particles, heat, and neutrons. Some other advantages might be discovered during the further analysis.

While this paper was under review, further calculations [19] via the 3D equilibrium code VMEC [20] showed a number of interesting results which we would like to mention here. It was found that addition of the plasma current in SS produces positive changes: The total rotational transform increases and the horizontal plasma position and the magnetic axis location can be effectively controlled by the currents in the PF coils. The high β equilibria [$\beta(0) > 30\%$] have been found in SS with the plasma current. It has been found also that the bootstrap effect can supply the

full plasma current required for the high β equilibria in SS. The particle transport is a very important issue as well, and the first step in such an analysis is to make a presentation of $|B|$ on the flux surfaces in Boozer coordinates. We did such calculations (by using S. Hirshman's code) and found [21], in particular, that the magnetic field in SS possesses a wonderful feature: At the average minor radius $\rho > \rho_{\max}/2$, the toroidal symmetry is more pronounced with increasing ρ . This means that the particle transport at $\rho > \rho_{\max}/2$ should be similar to that in ST, which is rather good. More detailed calculations are in progress.

The author would like to acknowledge valuable discussions with Joseph Talmadge and David Anderson and their cooperation on the UBFIELD code. Cooperation of Steve Hirshman in making his codes available is greatly appreciated. This work was supported by U.S. DOE Grants No. DE-FG02-88ER53264 and No. DE-FG02-88ER53263.

- [1] JET Team, J. Jacquinot *et al.*, Plasma Phys. Controlled Fusion **35**, A35 (1993).
- [2] TFTR Team, R.J. Hawryluk *et al.*, in *Proceedings of the 15th IAEA International Conference on Plasma Physics and Controlled Nuclear Fusion Research, Seville, Spain, 1994* (IAEA, Vienna, 1995), Vol. 1, p. 11.
- [3] JT-60 Team, M. Kikuchi *et al.*, in Ref. [2], p. 31.
- [4] A. Iiyoshi *et al.*, Fusion Technol. **17**, 169 (1990).
- [5] J. Kisslinger, C. D. Beidler, E. Harmeyer, F. Rau, H. Renner, and H. Wobig, in *Proceedings of the 22nd European Conference on Controlled Fusion and Plasma Physics, Bournemouth, England, 1995* (Plasma Fusion Center, MIT, Cambridge, MA, 1995), Vol. 19C, p. III-149.
- [6] A. Sykes *et al.*, in Ref. [2], Vol. 1, p. 719.
- [7] Y. S. Hwang *et al.*, in Ref. [2], Vol. 1, p. 737.
- [8] M. Ono *et al.*, Bull. Am. Phys. Soc. **40**, 1655 (1995).
- [9] K. Nishimura *et al.*, Fusion Technol. **17**, 86 (1990).
- [10] R. F. Gandy *et al.*, Fusion Technol. **18**, 281 (1990).
- [11] J. F. Lyon, B. A. Carreras, V. E. Lynch, J. S. Tolliver, and I. N. Sviatoslavsky, Fusion Technol. **15**, 1401 (1989).
- [12] B. A. Carreras *et al.*, Nucl. Fusion **28**, 1195 (1988).
- [13] J. F. Lyon *et al.*, Fusion Technol. **17**, 188 (1990).
- [14] P. E. Moroz, Phys. Plasmas **2**, 4269 (1995).
- [15] P. E. Moroz, Fusion Technology (to be published).
- [16] P. E. Moroz, in Ref. [5], p. II-049 (1995).
- [17] P. E. Moroz, Bull. Am. Phys. Soc. **40**, 1858 (1995).
- [18] L. S. Solov'ev and V. D. Shafranov, in *Reviews of Plasma Physics*, edited by M. A. Leontovich (Consultants Bureau, New York, 1970), Vol. 5, p. 1.
- [19] P. E. Moroz, Physics of Plasma (to be published).
- [20] S. P. Hirshman and D. K. Lee, Comput. Phys. Commun. **39**, 161 (1986).
- [21] P. E. Moroz, International Sherwood Fusion Theory Conference, Philadelphia (Report No. 3C26, 1996).